Supplementary Materials

Interface enhancement through electrostatic self-assembly for synergistically stabilized silicon anodes in lithium-ion batteries

Junfeng Shi, Siqi Hou, Weiyan Li, Dafang He, Maolei Huang, Jiawei Xia, Xingyue Qian*, Haiqun Chen*

Key Laboratory of Advanced Catalytic Materials and Technology, Advanced Catalysis and Green Manufacturing Collaborative Innovation Center, Changzhou University, Changzhou, Jiangsu Province 213164, China

Corresponding authors:

E-mail addresses: qianxy@cczu.edu.cn (X. Qian), chenhq@cczu.edu.cn (H. Chen)

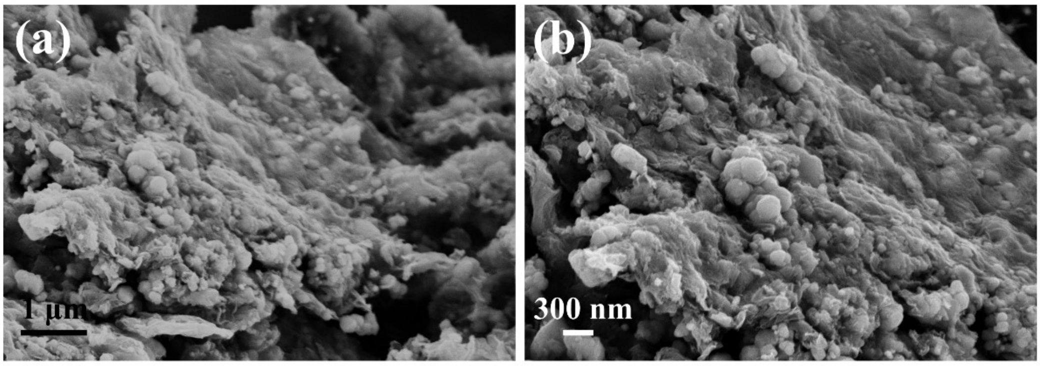

Fig. S1 SEM images of Si@RGO/C at different magnifications.

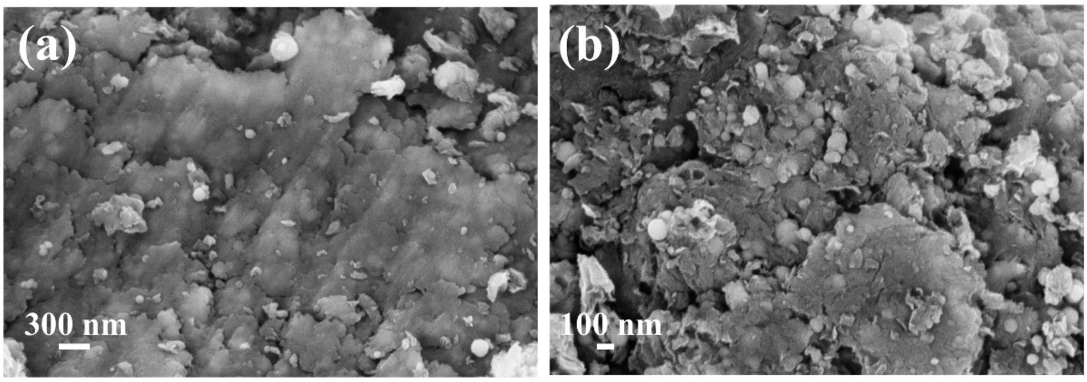

Fig. S2 SEM images of Si@PVP@RGO/C at different magnifications.

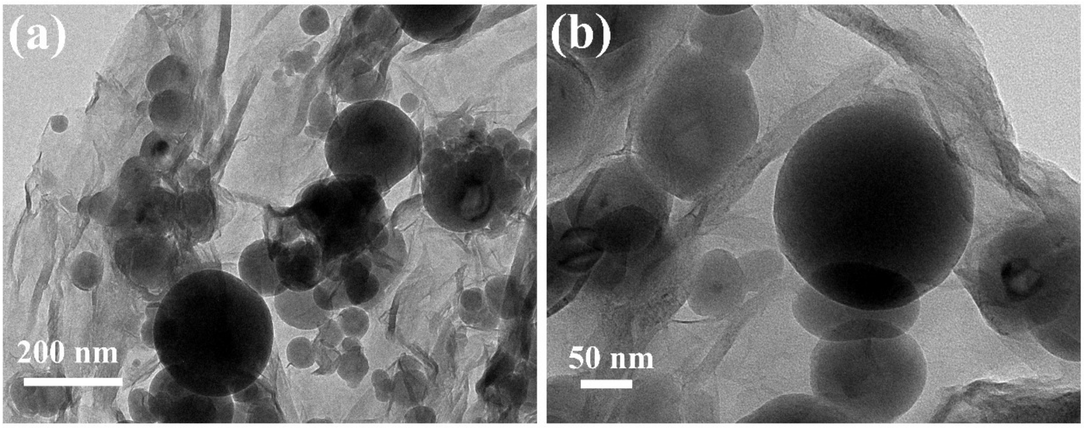

Fig. S3 TEM images of Si@PVP@RGO/C.

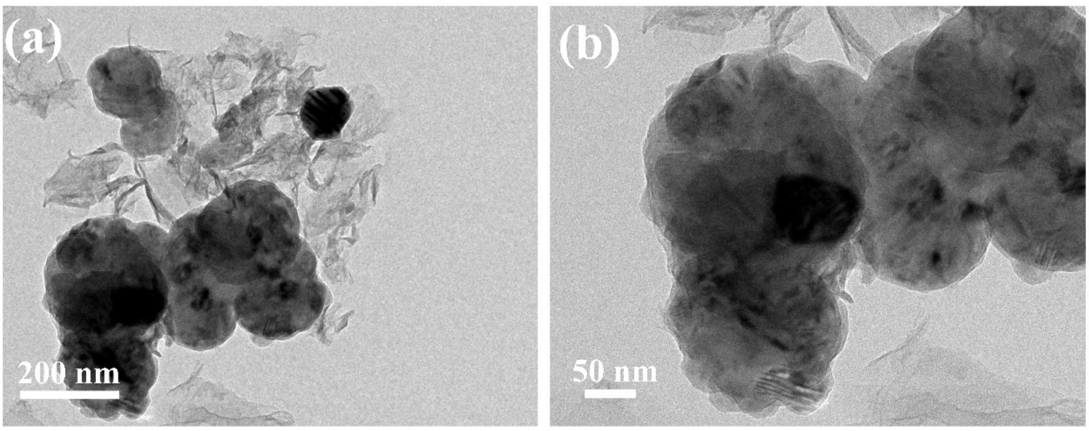

Fig. S4 TEM images of Si@RGO/C.

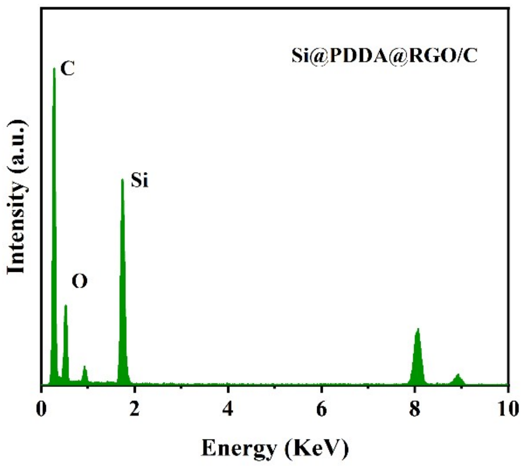

Fig. S5 EDX spectrum of Si@PDDA@RGO/C.

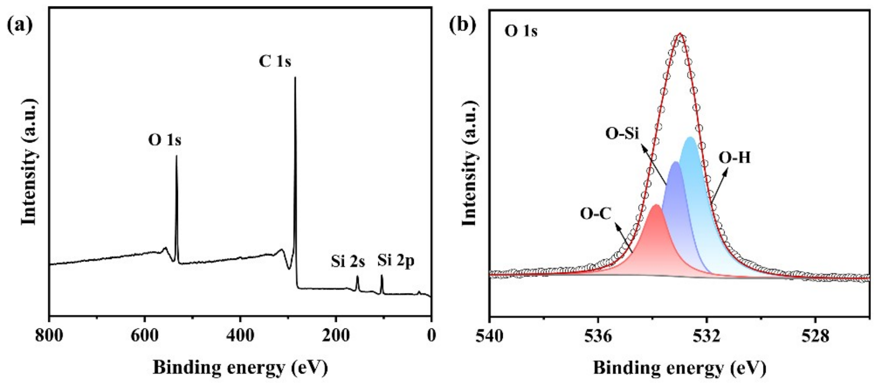

Fig. S6 (a) XPS survey spectra of Si@PDDA@RGO/C. (b) High-resolution curves of O 1s for Si@PDDA@RGO/C.

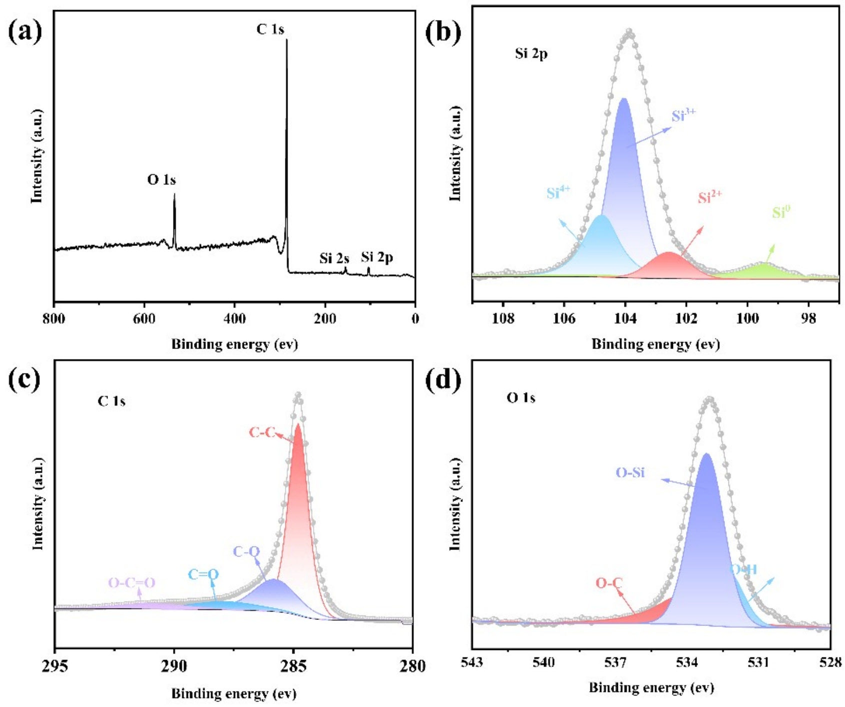

Fig. S7 (a) XPS survey spectrum of Si@PVP@RGO/C. The high-resolution spectra of (b) Si 2p, (c) C 1s, (d) O 1s for Si@PVP@RGO/C.

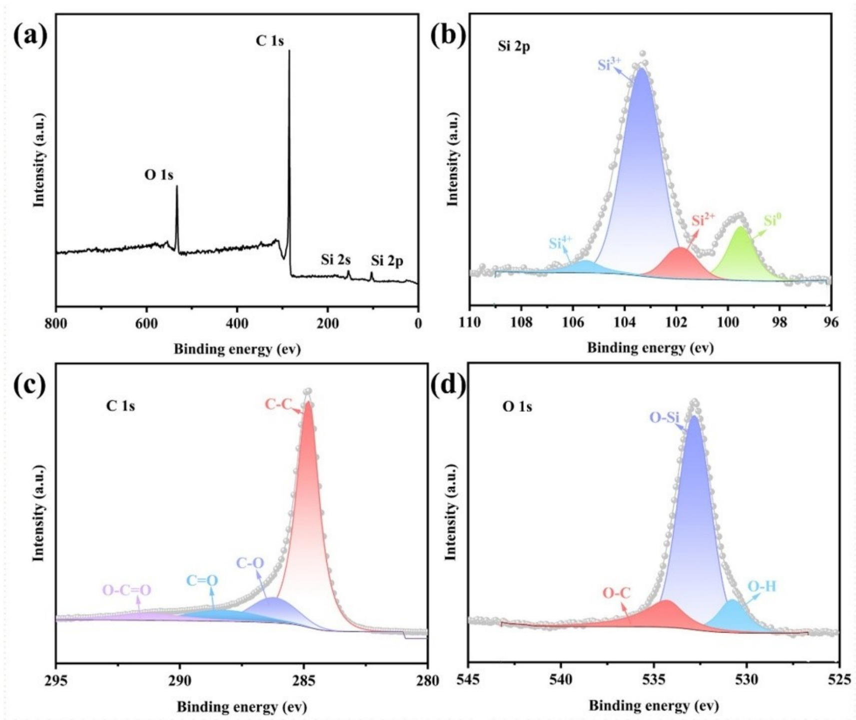

Fig. S8 (a) XPS survey spectrum of Si@RGO/C. The high-resolution spectra of (b) Si 2p, (c) C 1s, (d) O 1s for Si@RGO/C.

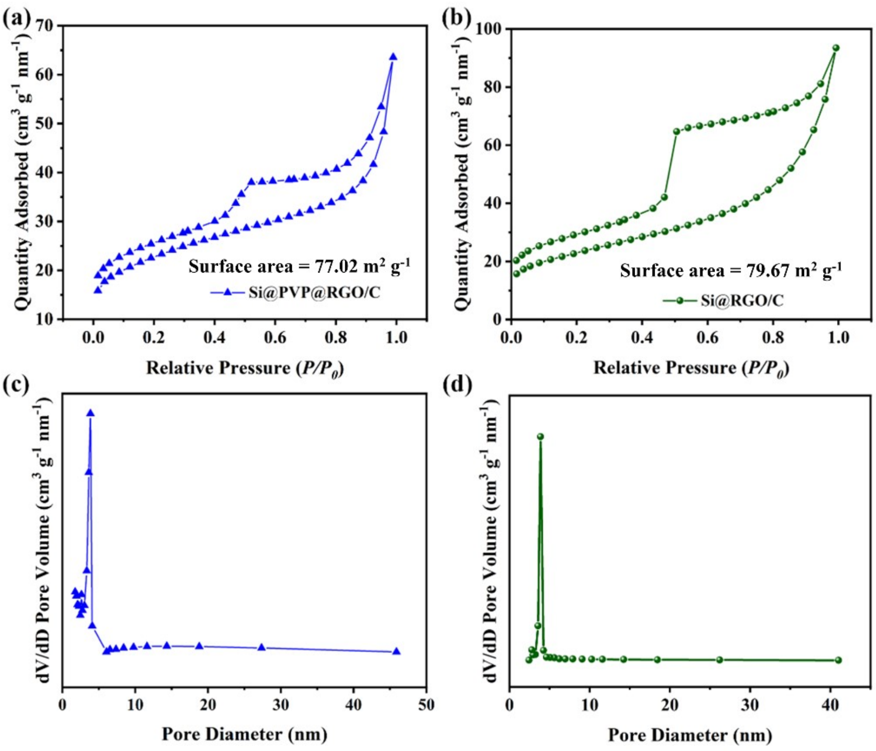

Fig. S9 (a, b) N_2 adsorption/desorption isotherms of Si@PVP@RGO/C and Si@RGO/C. (c, d) BJH pore size distribution plots of Si@PVP@RGO/C and Si@RGO/C.

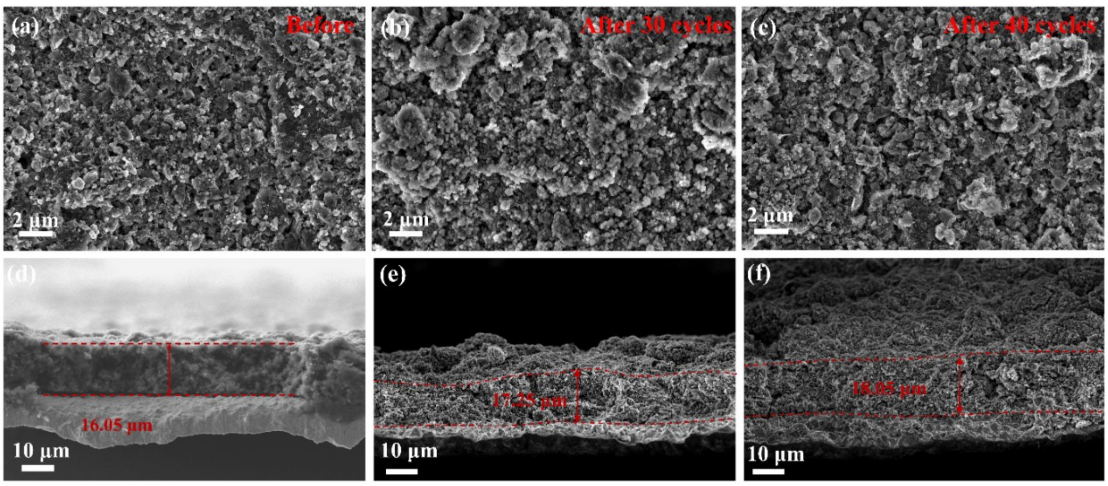

Fig. S10 Cross section and surface morphology of Si@PDDA@RGO/C anodes (a, d) before and after (b, e) 30 and (c, f) 40 cycles, respectively.

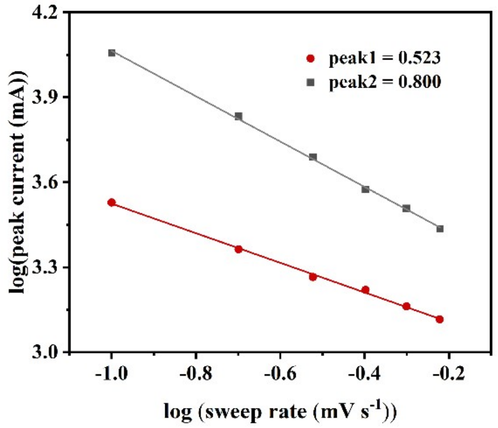

Fig. S11 The relationship between the peak current and scan rate of Si@PDDA@RGO/C.

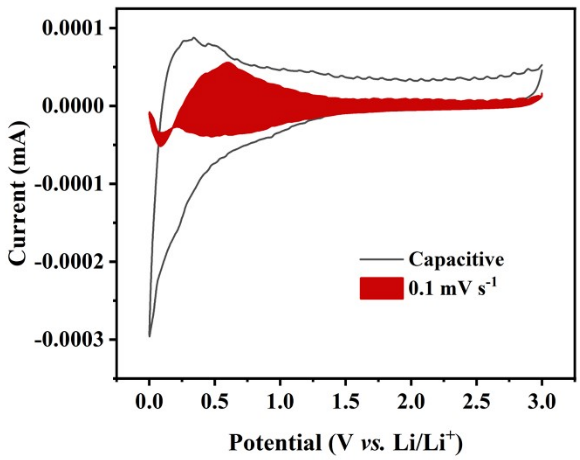

Fig. S12 Contribution of capacitance behavior for Si@PDDA@RGO/C at 0.1 mV s^{-1}.

Table S1 N_2 adsorption-desorption analysis of obtained samples.

Electrode material	Surface area (m^2 g^{-1})	Average pore diameter (nm)
Si@PDDA@RGO/C	78.61	6.19
Si@PVP@RGO/C	77.02	6.09
Si@RGO/C	79.67	5.23

Table S2 Comparison of Si@PDDA@RGO/C composites in reported literature to this work.

Electrode material	Current density (A g^{-1})	First cycle capacity (mAh g^{-1})	ICE (%)	N^{th} capacity (cycles)	Ref.
Si@PDDA@RGO/C	**0.2**	**783.48/1292.24**	**60.63**	**620.13**	**This work**
(Si/G/G)@C	0.1	782.1/860.4	90.9	584.2(200)	[1]
Si/NC	0.5	1394.4	/	563.7(300)	[2]
Si@ZIF-glass	1	627/1010	62	650(500)	[3]
Si@void@NC	0.2	1082.5/1449.9	74.6	697.7(100)	[4]
Si@void@C	0.05	1487/2094	71	628(100)	[5]
Si-C	0.1	/505	/	395(50)	[6]
Si@NC/Co/CNTs	1	937/1288	72.8	758(800)	[7]
Si@void@C	0.1	904.8/1193.8	75.79	627.5(100)	[8]
GPSCM	0.05	598/767	78	589(50)	[9]

Table S3 EIS fitting results for all composites

Electrode material	R_s (Ω)	R_{ct} (Ω)	$Б$ (Ω $s^{-1/2}$)	D_{Li^+} (cm^2 s^{-1})
Si@PDDA@RGO/C	2.09	124.60	105.26	2.51×10^{-18}
Si@PVP@RGO/C	2.92	375.40	347.45	2.30×10^{-19}
Si@RGO/C	6.27	579.20	351.6	2.25×10^{-19}

References

1 C.Y. Ni, C.D. Xia, W.P. Liu, W. Xu, Z.Q. Shan, X.X. Lei, H.Q. Qian and Z.D.Tao, Materials, 2024, **17**, 754.

2 Z.L. Xiao, Y.B. Xia, C. Wang, T.T. Zhao, Q.X. Yan, M.Z. Xiao, X.X. Peng and L.B. Song, Ionics, 2024, **30**, 1-12.

3 J.J. Yan, C.W. Gao, S.B. Qi, Z.J. Jiang, L.R. Jensen, H.B. Zhan, Y.F. Zhang and Y.Z. Yue, Nano Energ, 2022, **103**, 107779.

4 Y.B. Wei, Y.D. Huang, Y.F. Zeng, Y. Zhang, W.H. Cheng, W.C. Wang, D.Z. Jia, X.C. Tang and L. Wang, ACS Appl. Energy Mater, 2022, **5**, 1471-1477.

5 L.W. Su, J. Xie, Y.W. Yu, L.B. Wang, Y.H. Wang and M.M. Ren, Phys. Chem. Chem. Phys., 2015, **17**, 17562-17565.

6 J.Q. Zhang, Y.F. Chen, X.Q. Chen, T.Y. Feng, P.X. Yang and M.Z. An, Ionics, 2020, **26**, 5941-5950.

7 H. Luo, Q. Wang, Y.J. Wang, C.H.Y. Xu, B.Y. Wang, M. Wang, H. Wu and Y. Zhang, Appl. Surf. Sci, 2020, **529**, 147134.

8 X.L. Xie, P. Xiao, L. Pang, P. Zhou, Y.J. Li, J. Luo, J. Z. Xiong and Y. Li, J. Alloy. Compd., 2023, **931**, 167473.

9 W.F. Ren, Z.L. Zhang, Y.H. Wang, Q.Q. Tan, Z.Y. Zhong and F. Su, J. Mater. Chem. A, 2015, **3**, 5859-5865.